

Effects of the FCNC couplings in production of new heavy quarks within Z' models at the LHC

V. Çetinkaya*

Dumlupınar University, Department of Physics, 43100 Merkez, Kütahya, Turkey

V. Ari[†] and O. Çakır[‡]

Ankara University, Department of Physics, 06100 Tandoğan, Ankara, Turkey

Abstract

We study the flavor changing neutral current couplings of new heavy quarks through the Z' models at the LHC. We calculate the cross sections for the signal and the corresponding standard model background processes. Considering the present limits on the mass of new heavy quarks and the Z' boson, we performed an analysis to investigate the parameter space (mixing and mass) through different Z' models. For an FCNC mixing parameter $x = 0.1$ and the Z' mass $M_{Z'} = 2000$ GeV, and new heavy quark mass $m_{t'} = 700$ GeV at the LHC with $\sqrt{s} = 13$ TeV, we find the cross section for single production of new heavy quarks associated with top quarks as 5.8 fb, 3.3 fb, 1.5 fb and 1.2 fb within the Z'_η , Z'_ψ , Z'_{LP} and Z'_χ models, respectively. It is shown that the sensitivity would benefit from the flavor tagging.

PACS numbers: 12.60.Cn Extensions of electroweak gauge sector, 14.70.Pw Other gauge bosons, 14.65.Jk Other quarks

* volkan.cetinkaya@dpu.edu.tr

† vari@science.ankara.edu.tr

‡ ocakir@science.ankara.edu.tr

I. INTRODUCTION

Addition of new heavy quarks would require the extension of the flavor mixing in charged current interactions as well as the extension of Higgs sector in the standard model (SM). A large number of new heavy quark pairs can be produced through their colour charges at the Large Hadron Collider (LHC). However, due to the expected smallness of the mixing between the new heavy quarks and known quarks through charged current interactions, the production and decay modes can be effected by the flavor changing neutral current (FCNC) interactions. A new symmetry beyond the SM is expected to explain the smallness of these mixings. We may anticipate the discovery of new physics by observing the sizable anomalous couplings in the heavy quark sector. The couplings of the new heavy quarks can be enhanced to observable levels within some new physics models. Many extensions of the SM predict the extra gauge bosons, especially the Z' -boson has been the object of extensive phenomenological studies (see [1] and references therein). An extra $U(1)'$ gauge boson Z' can induce flavor changing neutral currents. In the models with an extra $U(1)'$ group the Z' boson can have tree-level or an effective $Z'qq'$ couplings, where q and q' are both the up-type quarks or down-type quarks.

The Z' models have some special names [2]: the Z'_η , Z'_χ and Z'_ψ models corresponding to the specific values of the mixing angle in the E_6 model have different couplings to the fermions, and the leptophobic Z'_{LP} model has the couplings to quarks but no couplings to leptons.

The ATLAS and CMS collaborations have performed extensive searches of new vector resonances at the LHC. We summarize briefly these searches, that exploited data from the pp run at $\sqrt{s} = 7$ TeV and $\sqrt{s} = 8$ TeV, as well as the corresponding constraints on Z' boson masses. The most stringent limits come from searches with leptonic final states ($Z' \rightarrow l^+l^-$): $M_{Z'_\chi} > 2620$ GeV [3] and $M_{Z'_\eta} > 1870$ GeV [4], $M_{Z'_\psi} > 2260$ GeV [5] (more recently $M_{Z'_\psi} > 2510$ GeV [3]) for the Z' boson predicted by the $U(1)'$ extensions, also extending to the mass limit of $M_{Z'_S} > 2900$ GeV [3, 6] for a gauge boson with sequential couplings. The results from ATLAS experiment exclude a leptophobic Z' decaying to $t\bar{t}$ with a mass less than 1740 GeV at 95% C.L. [7], while the CMS experiment excludes a top-color Z' decaying to $t\bar{t}$ with a mass less than 2100 GeV at 95% C.L. [8]. These searches assume rather narrow width for the Z' boson ($\Gamma_{Z'}/M_{Z'} = 0.012$). From the electroweak precision

data analysis, the improved lower limits on the Z' mass are given in the range $1100 - 1500$ GeV, which gives a limit on the $Z - Z'$ mixing about 10^{-3} [2]. The limits on the Z' boson mass favors higher center of mass energy collisions for direct observation of the signal. Using dilepton searches with LHC data, the dark matter constraints have been analysed in Ref. [9, 10] in the regime $M_{Z'} > 2m_{DM}$.

A work which addresses the effects of FCNC interactions induced by an additional Z' boson on the single top quark and top quark pair production at the LHC ($\sqrt{s} = 14$ TeV) has been performed in Ref. [11, 12]. The relevant signal cross sections have been calculated and especially the benefit from flavor tagging to identify the signal has been discussed. Considering an existence of sizeable couplings to the new heavy quarks, the Z' boson decay width and branchings, as well as the production rates, can be quite different from the expectations of usual search scenarios.

The new heavy quarks can be produced dominantly in pairs through strong interactions for masses around 1 TeV in the pp collisions of the LHC with a center of mass energy of 13 TeV. The single production of new heavy quarks would only be dominant over pair production for the large quark masses [13], it is model dependent, and it could be suppressed if the mixing with SM quarks is small.

There are searches for pair production and single production of new heavy quarks at the LHC. The ATLAS and CMS collaborations focused on decay modes assuming a 100% branching ratio of new heavy quarks, based on $L_{int} \approx 20 \text{ fb}^{-1}$ of pp collision data at $\sqrt{s} = 8$ TeV, and set lower mass limit for up type new heavy quark as $m_{t'} > 700$ GeV [14] and $m_{t'} > 735$ GeV [15].

In this work, we investigate the single production of new heavy quarks via FCNC interactions through Z' boson exchange at the LHC. The aim of this paper is to study the signal and background in detail within the same MC framework, therefore, we implement the related interaction vertices into the MC software. Another feature of the work is to analyze the signal observability (via contour plots) for different mass values of the Z' boson and new heavy quarks as well as the mixing parameter through FCNC interactions. In section II, we calculate the decay widths and branching ratios of Z' boson for the mass range $1500 - 3000$ GeV in the framework of different Z' models. An analysis of the parameter space of mass and coupling strength is given for the single production of new heavy quarks at the LHC in section III. We analyzed the signal observability for the $Z'qq'$ FCNC interactions. In order

to enrich the signal statistics even at the small couplings we consider both $t'\bar{t}$ and $\bar{t}'t$ single new heavy quark productions. The analysis for the signal significance is given in section IV and the work ends up with the conclusions as given in section V.

II. FCNC INTERACTIONS

In the gauge eigenstate basis, following the formalism given in Ref. [11, 16, 17], the additional neutral current Lagrangian associated with the $U(1)'$ gauge symmetry can be written as

$$\mathcal{L}' = -g' \sum_{f,f'} \bar{f} \gamma^\mu [\epsilon_L(f f') P_L + \epsilon_R(f f') P_R] f' Z'_\mu \quad (1)$$

where $\epsilon_{L,R}(f f')$ are the chiral couplings of Z' boson with fermions f and f' . The g' is the gauge coupling of the $U(1)'$, and $P_{R,L} = (1 \pm \gamma^5)/2$. Here, we assume that there is no mixing between the Z and Z' bosons as favored by the precision data. Flavor changing neutral currents (FCNCs) arise if the chiral couplings are nondiagonal matrices. In case the Z' couplings are diagonal but nonuniversal, flavor changing couplings are emerged by fermion mixing. In the interaction basis the FCNC for the up-type quarks are given by

$$\mathcal{J}_{FCNC}^u = (\bar{u}, \bar{c}, \bar{t}, \bar{t}') \gamma_\mu (\epsilon_L^u P_L + \epsilon_R^u P_R) \begin{pmatrix} u \\ c \\ t \\ t' \end{pmatrix}, \quad (2)$$

where the chiral couplings are given by

$$\epsilon_L^u = C_L^u \begin{pmatrix} 1 & 0 & 0 & 0 \\ 0 & 1 & 0 & 0 \\ 0 & 0 & 1 & 0 \\ 0 & 0 & 0 & x \end{pmatrix} \quad \text{and} \quad \epsilon_R^u = C_R^u \begin{pmatrix} 1 & 0 & 0 & 0 \\ 0 & 1 & 0 & 0 \\ 0 & 0 & 1 & 0 \\ 0 & 0 & 0 & 1 \end{pmatrix}. \quad (3)$$

In general, the effects of these FCNCs may occur both in the up-type sector and down-type sector after diagonalizing their mass matrices. For the right-handed up-sector and down-sector one assumes that the neutral current couplings to Z' are family universal and flavor diagonal in the interaction basis. In this case, unitary rotations ($V_{L,R}^f$) can keep the

right handed couplings flavor diagonal, and left handed sector becomes nondiagonal. The chiral couplings of Z' in the fermion mass eigenstate basis are given by

$$B_L^{ff'} \equiv V_L^f \epsilon_L^u (ff') V_L^{f^\dagger} \quad \text{and} \quad B_R^{ff'} \equiv V_R^f \epsilon_R^u (ff') V_R^{f^\dagger}. \quad (4)$$

Here the matrix can be written as $V' = V_L^u V_L^{d^\dagger}$ with the assumption that the down-sector has no mixing. The flavor mixing in the left-handed quark fields is simply related to V' , assuming the up sector diagonalization and unitarity of the CKM matrix one can find the couplings $B_L^u \equiv V_{uL}^\dagger \epsilon_L^u V_{uL} = V' \epsilon_L^u V'^\dagger$ with the parametrization $|V_{iQ}| = |A_{iQ}| \lambda^{4-i}$ for the matrix, where the generation index i runs from 1 to 3.

The FCNC effects from the Z' mediation have been studied for the down-type sector and implications in flavor physics through B -meson decays [18–23] and B -meson mixing [17, 24–28]. These effects have also been studied for up-type quark sector in top quark production [11, 29–33]. The parameters for different Z' models are given in Table I. In numerical calculations, we take the coupling $g' \simeq 0.40$ for the models.

In our model, the chiral couplings can be written as

$$B_L^u \approx C_L^u \begin{pmatrix} 1 + (x-1) |A_{14}|^2 \lambda^6 & (x-1) A_{14} A_{24}^* \lambda^5 & (x-1) A_{14} A_{34}^* \lambda^4 & (x-1) A_{14} A_{44}^* \lambda^3 \\ (x-1) A_{24} A_{14}^* \lambda^5 & 1 + (x-1) |A_{24}|^2 \lambda^4 & (x-1) A_{24} A_{34}^* \lambda^3 & (x-1) A_{24} A_{44}^* \lambda^2 \\ (x-1) A_{34} A_{14}^* \lambda^4 & (x-1) A_{34} A_{24}^* \lambda^3 & 1 + (x-1) |A_{34}|^2 \lambda^2 & (x-1) A_{34} A_{44}^* \lambda^1 \\ (x-1) A_{44} A_{14}^* \lambda^3 & (x-1) A_{44} A_{24}^* \lambda^2 & (x-1) A_{44} A_{34}^* \lambda^1 & 1 + (x-1) |A_{44}|^2 \end{pmatrix} \quad (5)$$

The values of the matrix elements $|A_{14}| = 3.2$, $|A_{24}| = 2.0$ and $|A_{34}| = 3.0$ are used as given in Ref. [34] by taking into account $\lambda = 0.22$. For a comparison, we also calculate the cross sections using the scenario of equal parameters $|A_{i4}| = 2.0$ (where i runs from 1 to 3).

III. SINGLE PRODUCTION OF NEW HEAVY QUARKS

For numerical calculations we have implemented the $Z'qq'$ interaction vertices into the CalcHEP program package [35]. The decay widths of Z' boson for different mass values within different Z' models are given in Table II. For the parameter $x = 1$, both the left-handed and right-handed couplings become universal, and family diagonal. In this case we cannot see the FCNC effects on the decay widths and cross sections. For the FCNC

Table I. The chiral couplings of Z' boson with quarks and leptons predicted by different models.

	Z'_χ	Z'_ψ	Z'_η	Z'_{LP}
Q_L^u	$-1/2\sqrt{10}$	$1/\sqrt{24}$	$-1/\sqrt{15}$	$1/9$
Q_R^u	$1/2\sqrt{10}$	$-1/\sqrt{24}$	$1/\sqrt{15}$	$-8/9$
Q_L^d	$-1/2\sqrt{10}$	$1/\sqrt{24}$	$-1/\sqrt{15}$	$1/9$
Q_R^d	$-3/2\sqrt{10}$	$-1/\sqrt{24}$	$-1/2\sqrt{15}$	$1/9$
Q_L^e	$3/2\sqrt{10}$	$1/\sqrt{24}$	$1/2\sqrt{15}$	0
Q_R^e	$1/2\sqrt{10}$	$-1/\sqrt{24}$	$1/\sqrt{15}$	0
Q_L^ν	$3/2\sqrt{10}$	$1/\sqrt{24}$	$1/2\sqrt{15}$	0

effects on the decay width, we take the parameter $x = 0.1$ as shown in Fig. 1. All these scenarios of Z' models predict a narrow decay width ranging from 0.6% to 3% for $\Gamma_{Z'}/M_{Z'}$ depending on the mass of Z' boson foreseen by different models, for the considered set of parameters. The effect of the FCNC reduces the decay width in the relevant mass range. The decay widths are compared with the similar results from Ref. [11, 12] for $x = 0.1$ to prove the implementation. The branching ratios of Z' boson decays depending on its mass predicted by different Z' models are given in Fig. 2 - Fig. 9, specifically they are given in Fig. 2, Fig. 4 and Fig. 6 for the diagonal couplings to quarks and leptons, while they are given in Fig. 3, Fig. 5 and Fig. 7 for the FCNC couplings to different flavors of up sector quarks within the Z'_η , Z'_χ and Z'_ψ models, respectively. In Fig. 8 and Fig. 9, the branchings for a leptophobic Z'_{LP} boson decays to pair of quarks with diagonal couplings and FCNC couplings are presented depending on its mass.

The cross sections for the process $pp \rightarrow (t\bar{t} + \bar{t}'t) + X$ depending on the Z' boson mass at the LHC ($\sqrt{s} = 13$ TeV) are given in Fig. 10 and Fig. 11 by using parton distribution function library CTEQ6L [36]. Here, the Z' boson contributes through the s - and t -channel diagrams, and the cross sections of associated production of single top quarks and single new heavy quarks ($t\bar{t}$ and $\bar{t}'t$) in the final state are summed. For this process the cross section at $\sqrt{s} = 13$ TeV is about 8 times larger than the case at $\sqrt{s} = 8$ TeV.

Fig. 12 shows the p_T distributions of the b -quark in the signal process with $M_{Z'} = 1500$ GeV for the parameter $x = 0.1$ at the pp center of mass energy of 13 TeV. A high p_T cut reduces the background significantly without affecting much the signal cross section in the

Table II. The total decay widths of Z' boson for different mass in various models with the FCNC parameter $x = 0.1$.

$M_{Z'}(\text{GeV})$	$\Gamma(Z'_\chi)(\text{GeV})$	$\Gamma(Z'_\psi)(\text{GeV})$	$\Gamma(Z'_\eta)(\text{GeV})$	$\Gamma(Z'_{LP})(\text{GeV})$
1400	17.25	7.73	9.21	28.85
1600	21.75	9.20	11.61	37.44
1800	25.11	10.66	13.46	43.99
2000	28.30	12.11	15.22	50.25
2200	31.41	13.55	16.95	56.36
2400	34.48	14.98	18.65	62.36
2600	37.53	16.40	20.33	68.30
2800	40.55	17.82	22.01	74.18
3000	43.56	19.23	23.67	80.02

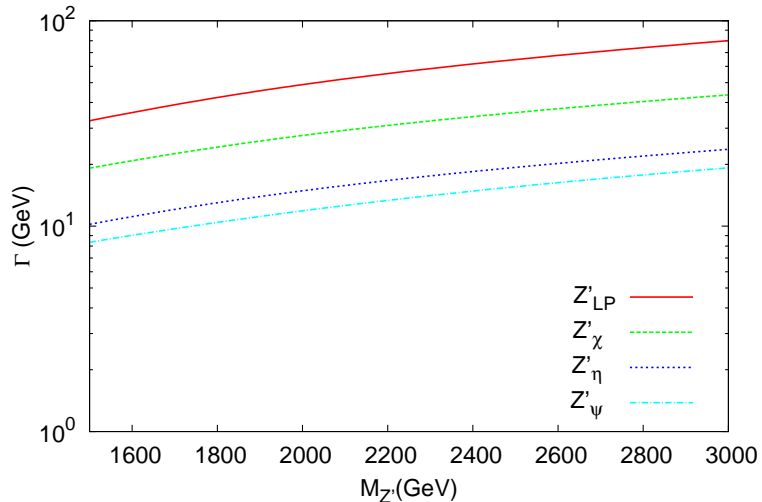


Figure 1. The decay widths of Z' boson depending on its mass for different Z' models with the FCNC parameter $x = 0.1$.

interested Z' mass range. The rapidity distribution of the bottom quarks (b and \bar{b}) from the signal are shown in Fig. 13 at the collision energy of 13 TeV. In order to enhance the statistics we sum up the b and \bar{b} distributions. There is a peak in the b -quark rapidity distribution $\eta^b \simeq 0$ with the tails extending to $|\eta^b| \simeq 2.5$. For the analysis, the suitable cuts are $p_T^{b,\bar{b}} > 100$ GeV, $|\eta^{b,\bar{b}}| \leq 2.0$ and $m_{Wb} > 400$ GeV. The cut m_{Wb} is also useful well above the top quark

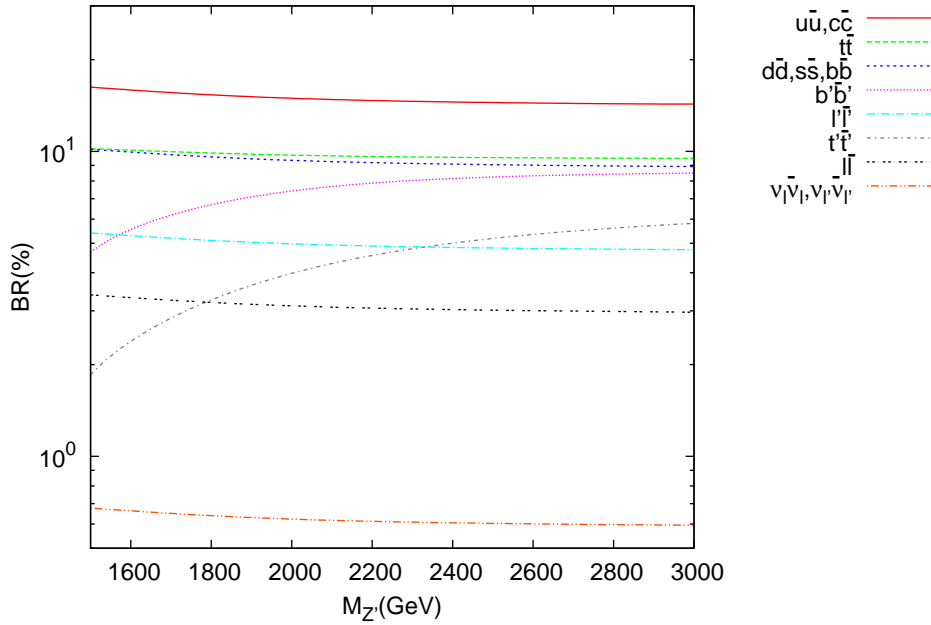


Figure 2. Branching ratios (%) depending on the mass of Z' boson for diagonal couplings to quarks and leptons within the Z'_η model.

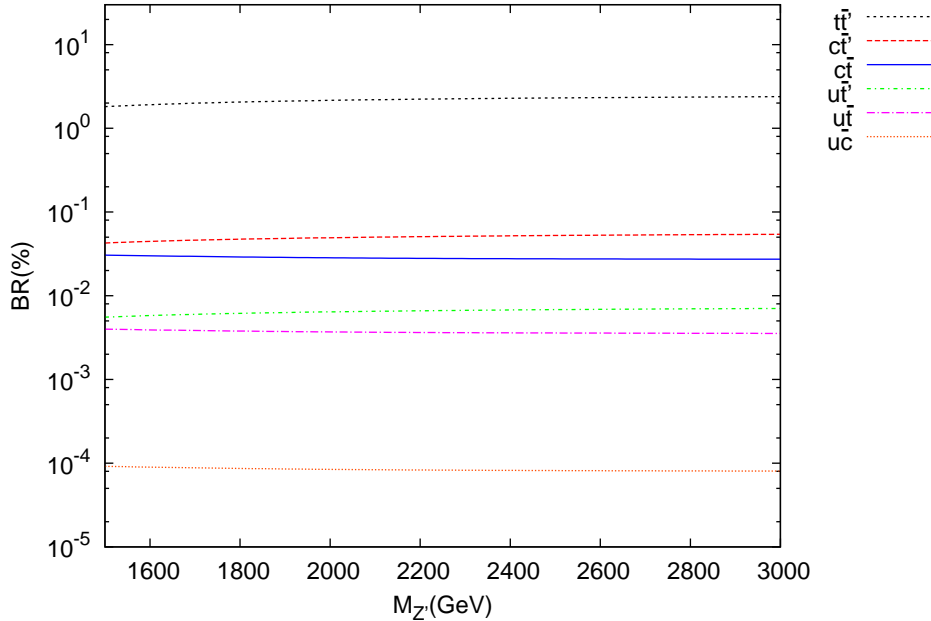


Figure 3. Branching ratios (%) depending on the mass of the Z' boson for FCNC couplings to different flavors of up sector quarks within the Z'_η model.

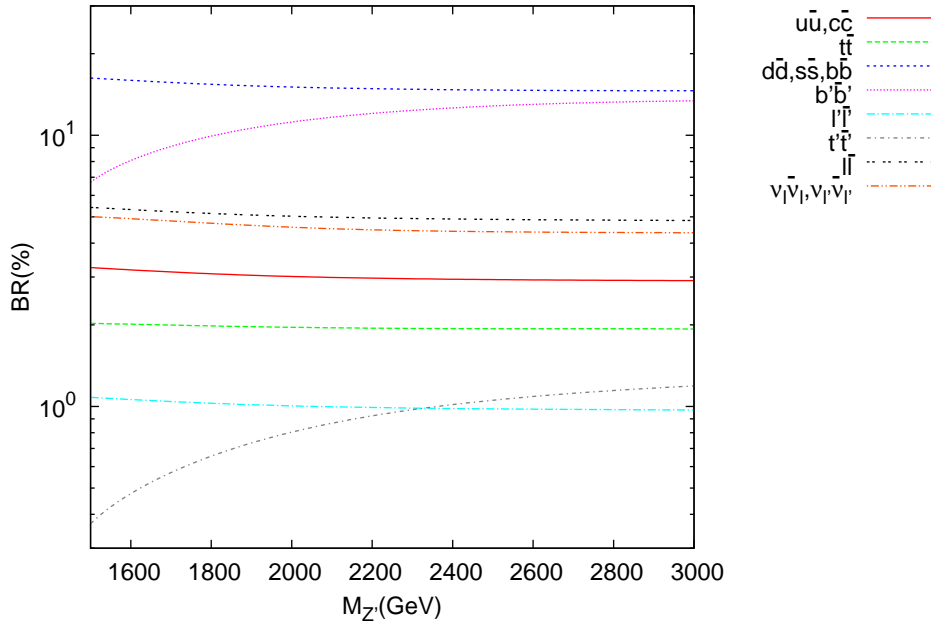


Figure 4. Branching ratios (%) depending on the mass of Z' boson for diagonal couplings to quarks and leptons within the Z'_χ model.

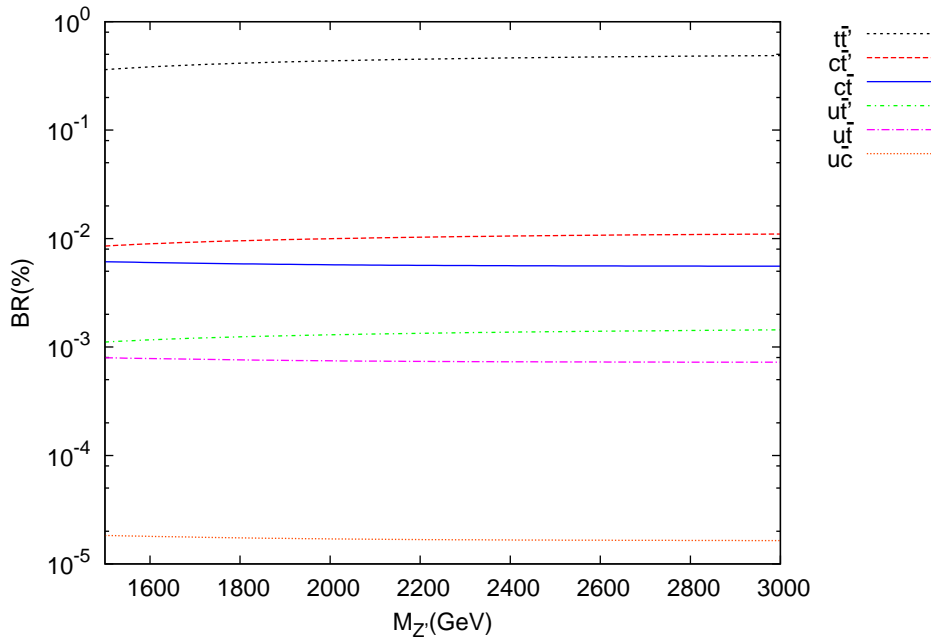


Figure 5. Branching ratios (%) depending on the mass of the Z' boson for FCNC couplings to different flavors of up sector quarks within the Z'_χ model.

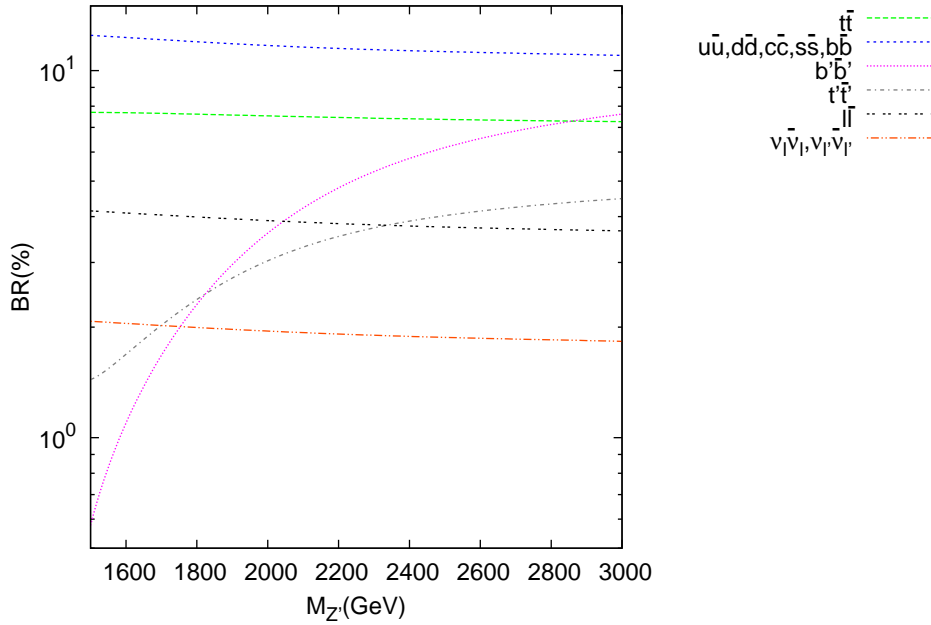


Figure 6. Branching ratios (%) depending on the mass of Z' boson for diagonal couplings to quarks and leptons within the Z'_ψ model.

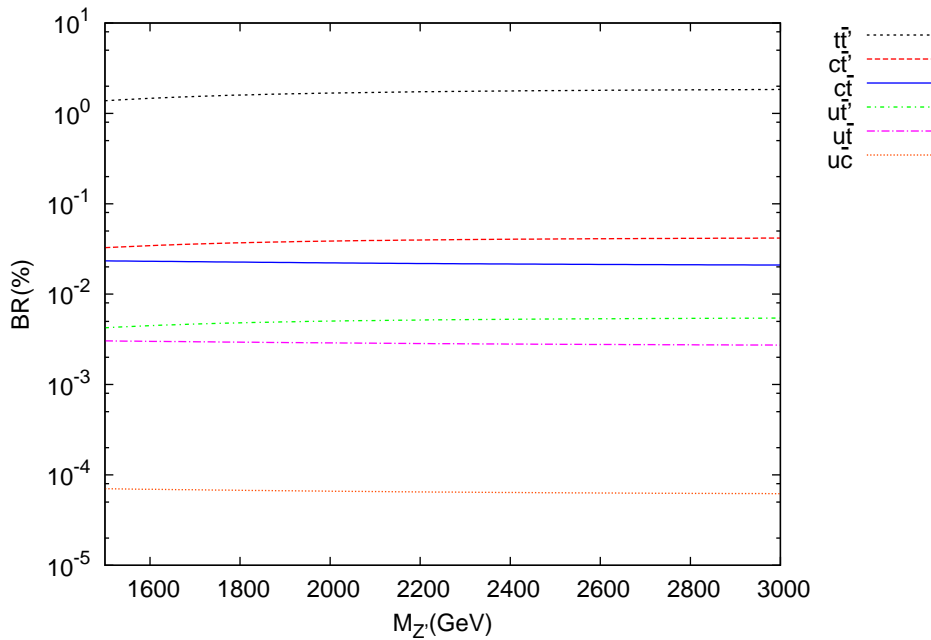


Figure 7. Branching ratios (%) depending on the mass of the Z' boson for FCNC couplings to different flavors of up sector quarks within the Z'_ψ model.

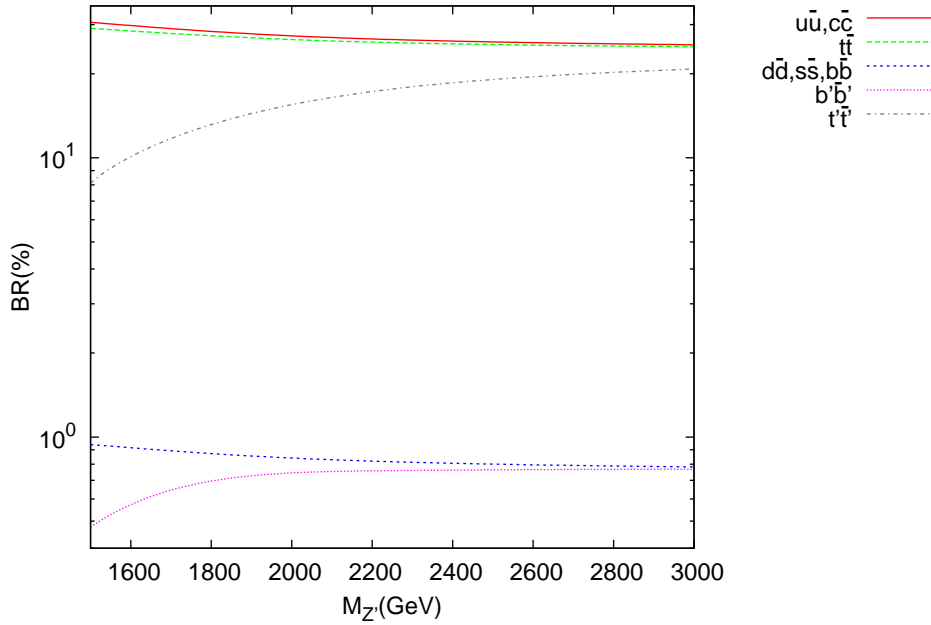


Figure 8. Branching ratios (%) depending on the mass of Z' boson for diagonal couplings to quarks within the Z'_{LP} model.

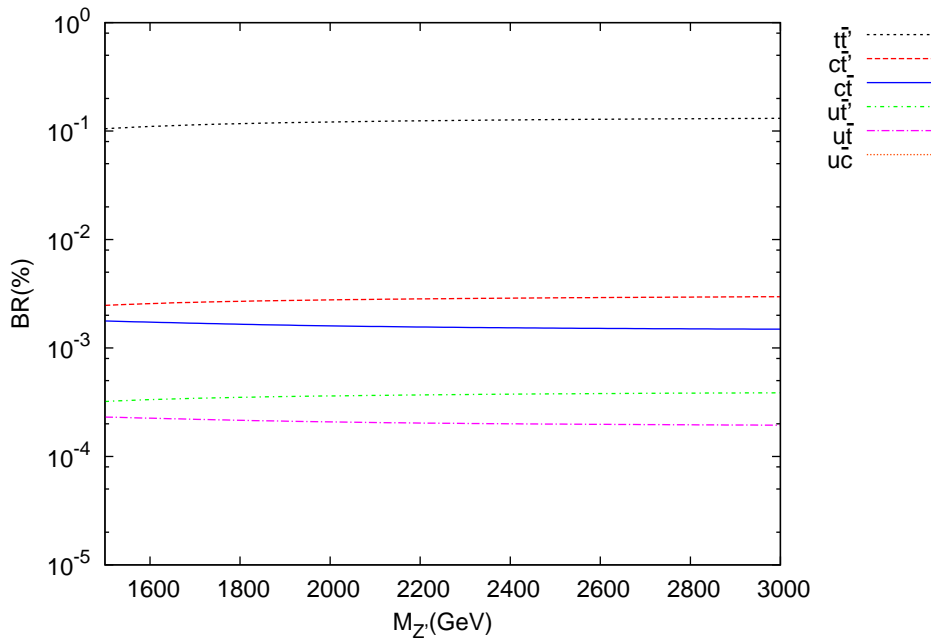


Figure 9. Branching ratios (%) depending on the mass of the Z' boson for FCNC couplings to different flavors of up sector quarks within the Z'_{LP} model.

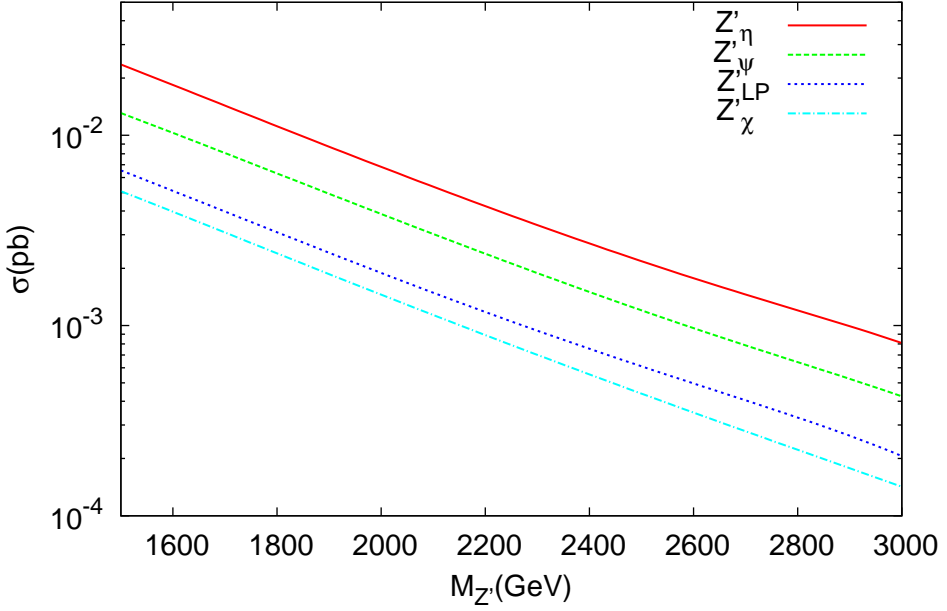


Figure 10. The cross sections for $pp \rightarrow (t'\bar{t} + \bar{t}'t) + X$ versus the Z' boson mass at the LHC with $\sqrt{s} = 13$ TeV. The lines are for different Z' models as explained in the text, where the parameters $A_{14} = A_{41} = 3.2$, $A_{24} = A_{42} = 2.0$ and $A_{34} = A_{43} = 3.0$ are used.

mass. We also apply invariant mass cut (for Wbt system) $M_{Z'} - 4\Gamma_{Z'} < m_{Wbt} < M_{Z'} + 4\Gamma$ to make analysis with the signal and background.

The signal cross sections (σ_S) in the invariant mass interval of $M_{Z'} - 4\Gamma_{Z'} < m_{Wbt} < M_{Z'} + 4\Gamma$, for the process $pp \rightarrow (W^+b\bar{t} + W^-b\bar{t}) + X$ are given in Table III, Table IV, Table V and Table VI for different values of FCNC parameter x (ranging from 0.01 to 0.5) within the Z'_η (Z'_χ) model, where new heavy quark masses are taken 600 GeV, 700 GeV and 800 GeV. For the Z'_ψ (Z'_LP) model and the FCNC parameter for 0.01, 0.05, 0.1 and 0.5, the cross sections (σ_S) are presented in Table VII, Table VIII, Table IX and Table X, respectively. The cross section for the corresponding background are given in Table XI for the chosen invariant mass interval.

We plot the invariant mass distribution of the Wbt system for the signal (with $x = 0.1$ and $m_{t'} = 700$ GeV) and background at the LHC with $\sqrt{s} = 13$ TeV in Fig. 14, Fig. 15, Fig. 16 and Fig. 17 for different Z' models.

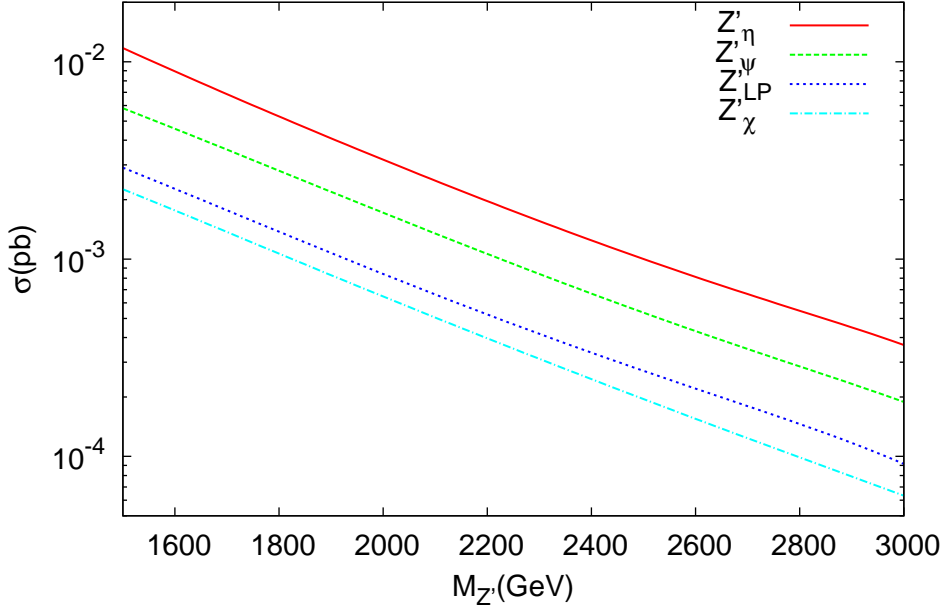


Figure 11. The cross sections for $pp \rightarrow (t't + t't) + X$ versus the Z' boson mass at the LHC with $\sqrt{s} = 13$ TeV. The lines are for the four Z' models as explained in the text and the values of parameters $A_{i4} = A_{4i} = 2$ (where i runs from 1 to 3) are used.

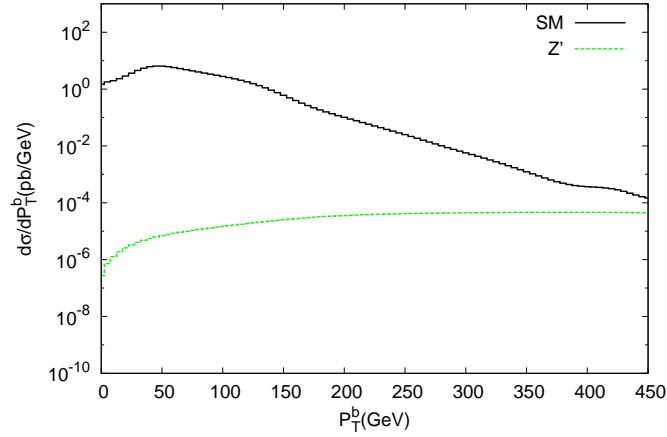


Figure 12. The transverse momentum (p_T) distribution of the bottom quarks (b and \bar{b}) for the signal and background processes $pp \rightarrow (W^+ b \bar{b} + W^- \bar{b} b) + X$ at the LHC with $\sqrt{s} = 13$ TeV for the FCNC parameter $x = 0.1$. These results are obtained for the Z'_η model.

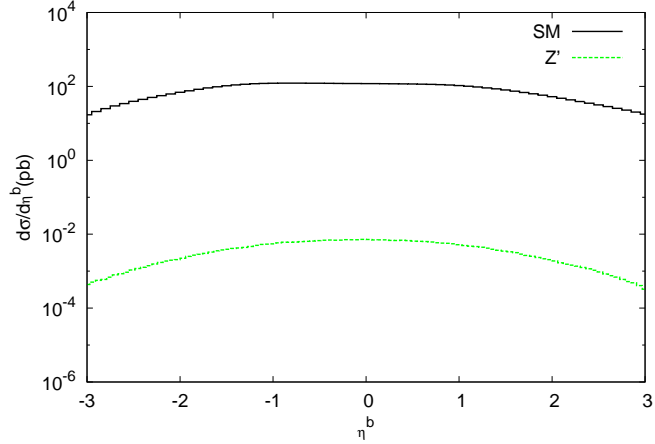


Figure 13. The pseudo-rapidity distribution of the bottom quarks (b and \bar{b}) for the signal (Z') and background processes (SM) $pp \rightarrow (W^+b\bar{t} + W^-\bar{b}t) + X$ at the LHC with $\sqrt{s} = 13$ TeV. The results are obtained for the Z'_η model.

Table III. The total cross section for the signal (σ_S) depending on the Z' boson mass, these values are calculated for the process $pp \rightarrow (W^+b\bar{t} + W^-\bar{b}t) + X$ at the LHC with $\sqrt{s} = 13$ TeV. The results are obtained for the Z'_η model (the Z'_χ model) with the FCNC parameter $x = 0.01$.

σ_S (pb)			
$M_{Z'}$ (GeV)	$m_{t'} = 600$ GeV	$m_{t'} = 700$ GeV	$m_{t'} = 800$ GeV
1500	2.44×10^{-2} (5.51×10^{-3})	2.23×10^{-2} (4.98×10^{-3})	1.98×10^{-2} (4.41×10^{-3})
2000	7.31×10^{-3} (1.60×10^{-3})	6.95×10^{-3} (1.51×10^{-3})	6.49×10^{-3} (1.41×10^{-3})
2500	2.40×10^{-3} (5.05×10^{-4})	2.33×10^{-3} (4.90×10^{-4})	2.24×10^{-3} (4.70×10^{-4})
3000	1.01×10^{-3} (1.74×10^{-4})	9.93×10^{-4} (1.71×10^{-4})	9.71×10^{-4} (1.67×10^{-4})

Table IV. The same as Table III, but for $x = 0.05$.

σ_S (pb)			
$M_{Z'}$ (GeV)	$m_{t'} = 600$ GeV	$m_{t'} = 700$ GeV	$m_{t'} = 800$ GeV
1500	2.26×10^{-2} (5.06×10^{-3})	2.06×10^{-2} (4.59×10^{-3})	1.82×10^{-2} (4.07×10^{-3})
2000	6.75×10^{-3} (1.47×10^{-3})	6.44×10^{-3} (1.40×10^{-3})	6.00×10^{-3} (1.29×10^{-3})
2500	2.22×10^{-3} (4.65×10^{-4})	2.16×10^{-3} (4.51×10^{-4})	2.07×10^{-3} (4.32×10^{-4})
3000	9.28×10^{-4} (1.60×10^{-4})	9.17×10^{-4} (1.58×10^{-4})	8.96×10^{-4} (1.54×10^{-4})

Table V. The same as Table III, but for $x = 0.1$.

$M_{Z'}(\text{GeV})$	$\sigma_S(\text{pb})$		
	$m_{t'} = 600 \text{ GeV}$	$m_{t'} = 700 \text{ GeV}$	$m_{t'} = 800 \text{ GeV}$
1500	$2.04 \times 10^{-2} (4.55 \times 10^{-3})$	$1.86 \times 10^{-2} (4.12 \times 10^{-3})$	$1.64 \times 10^{-2} (3.66 \times 10^{-3})$
2000	$6.10 \times 10^{-3} (1.32 \times 10^{-3})$	$5.81 \times 10^{-3} (1.25 \times 10^{-3})$	$5.42 \times 10^{-3} (1.16 \times 10^{-3})$
2500	$2.00 \times 10^{-3} (4.19 \times 10^{-4})$	$1.95 \times 10^{-3} (4.05 \times 10^{-4})$	$1.87 \times 10^{-3} (3.89 \times 10^{-4})$
3000	$8.34 \times 10^{-4} (1.44 \times 10^{-4})$	$8.23 \times 10^{-4} (1.42 \times 10^{-4})$	$8.04 \times 10^{-4} (1.38 \times 10^{-4})$

 Table VI. The same as Table III, but for $x = 0.5$.

$M_{Z'}(\text{GeV})$	$\sigma_S(\text{pb})$		
	$m_{t'} = 600 \text{ GeV}$	$m_{t'} = 700 \text{ GeV}$	$m_{t'} = 800 \text{ GeV}$
1500	$6.45 \times 10^{-3} (1.41 \times 10^{-3})$	$5.85 \times 10^{-3} (1.28 \times 10^{-3})$	$5.09 \times 10^{-3} (1.13 \times 10^{-3})$
2000	$1.91 \times 10^{-3} (4.09 \times 10^{-4})$	$1.82 \times 10^{-3} (3.89 \times 10^{-4})$	$1.71 \times 10^{-3} (3.61 \times 10^{-4})$
2500	$6.22 \times 10^{-4} (1.30 \times 10^{-4})$	$6.09 \times 10^{-4} (1.26 \times 10^{-4})$	$5.87 \times 10^{-4} (1.20 \times 10^{-4})$
3000	$2.55 \times 10^{-4} (4.43 \times 10^{-5})$	$2.51 \times 10^{-4} (4.36 \times 10^{-5})$	$2.47 \times 10^{-4} (4.26 \times 10^{-5})$

IV. ANALYSIS

Here, we consider two types of backgrounds for the analysis. The first one has the same final state (Wbt) as expected for the signal processes and the other one (pair production of top quarks both associated with b -jets) is the irreducible background and contributes to

Table VII. The total cross section values for the signal (σ_S) are calculated for the process $pp \rightarrow (W^+b\bar{t} + W^-b\bar{t}) + X$ at the LHC with $\sqrt{s} = 13 \text{ TeV}$. The results are obtained for the Z'_ψ model (the Z'_{LP} model) and the FCNC parameter $x = 0.01$.

$M_{Z'}(\text{GeV})$	$\sigma_S(\text{pb})$		
	$m_{t'} = 600 \text{ GeV}$	$m_{t'} = 700 \text{ GeV}$	$m_{t'} = 800 \text{ GeV}$
1500	$1.42 \times 10^{-2} (6.22 \times 10^{-3})$	$1.28 \times 10^{-2} (5.77 \times 10^{-3})$	$1.08 \times 10^{-2} (5.20 \times 10^{-3})$
2000	$4.13 \times 10^{-3} (1.84 \times 10^{-3})$	$3.97 \times 10^{-3} (1.77 \times 10^{-3})$	$3.72 \times 10^{-3} (1.67 \times 10^{-3})$
2500	$1.33 \times 10^{-3} (6.13 \times 10^{-4})$	$1.30 \times 10^{-3} (6.01 \times 10^{-4})$	$1.26 \times 10^{-3} (5.82 \times 10^{-4})$
3000	$5.24 \times 10^{-4} (3.00 \times 10^{-4})$	$5.20 \times 10^{-4} (3.00 \times 10^{-4})$	$5.13 \times 10^{-4} (2.95 \times 10^{-4})$

Table VIII. The same as Table VII, but for $x = 0.05$.

$M_{Z'}(\text{GeV})$	$\sigma_S(\text{pb})$		
	$m_{t'} = 600 \text{ GeV}$	$m_{t'} = 700 \text{ GeV}$	$m_{t'} = 800 \text{ GeV}$
1500	$1.31 \times 10^{-2} (5.72 \times 10^{-3})$	$1.18 \times 10^{-2} (5.33 \times 10^{-3})$	$9.90 \times 10^{-3} (4.79 \times 10^{-3})$
2000	$3.82 \times 10^{-3} (1.70 \times 10^{-3})$	$3.67 \times 10^{-3} (1.64 \times 10^{-3})$	$3.43 \times 10^{-3} (1.55 \times 10^{-3})$
2500	$1.23 \times 10^{-3} (5.64 \times 10^{-4})$	$1.20 \times 10^{-3} (5.54 \times 10^{-4})$	$1.17 \times 10^{-3} (5.35 \times 10^{-4})$
3000	$4.84 \times 10^{-4} (1.77 \times 10^{-4})$	$5.21 \times 10^{-4} (2.76 \times 10^{-4})$	$4.72 \times 10^{-4} (2.72 \times 10^{-4})$

 Table IX. The same as Table VII, but for $x = 0.1$.

$M_{Z'}(\text{GeV})$	$\sigma_S(\text{pb})$		
	$m_{t'} = 600 \text{ GeV}$	$m_{t'} = 700 \text{ GeV}$	$m_{t'} = 800 \text{ GeV}$
1500	$1.18 \times 10^{-2} (5.17 \times 10^{-3})$	$1.06 \times 10^{-2} (4.78 \times 10^{-3})$	$8.93 \times 10^{-3} (4.30 \times 10^{-3})$
2000	$3.43 \times 10^{-3} (1.53 \times 10^{-3})$	$3.30 \times 10^{-3} (1.47 \times 10^{-3})$	$3.10 \times 10^{-3} (1.39 \times 10^{-3})$
2500	$1.11 \times 10^{-3} (5.06 \times 10^{-4})$	$1.09 \times 10^{-3} (4.97 \times 10^{-4})$	$1.05 \times 10^{-3} (4.82 \times 10^{-4})$
3000	$4.33 \times 10^{-4} (2.49 \times 10^{-4})$	$4.31 \times 10^{-4} (2.48 \times 10^{-4})$	$4.24 \times 10^{-4} (2.44 \times 10^{-4})$

the similar final state. The ratio of the cross sections for pair production of top quarks at the $\sqrt{s} = 13 \text{ TeV}$ and $\sqrt{s} = 8 \text{ TeV}$ is about 3.5. The ratio of the cross sections for process $pp \rightarrow (t'\bar{t} + t\bar{t}') + X$ is found to be about 8 for considered Z' models. It is expected that an improvement in the statistical significance (for the center of mass energy $\sqrt{s} = 13 \text{ TeV}$ when compared to the case of $\sqrt{s} = 8 \text{ TeV}$) will be obtained. For the analysis, one can apply a high transverse momentum (p_T) cut for the b -jets and the other jets. Employing the variable p_T cuts such that $p_T > 100 \text{ GeV}$ for different Z' mass values and the rapidity

 Table X. The same as Table VII, but for $x = 0.5$.

$M_{Z'}(\text{GeV})$	$\sigma_S(\text{pb})$		
	$m_{t'} = 600 \text{ GeV}$	$m_{t'} = 700 \text{ GeV}$	$m_{t'} = 800 \text{ GeV}$
1500	$3.72 \times 10^{-3} (1.60 \times 10^{-3})$	$3.34 \times 10^{-3} (1.49 \times 10^{-3})$	$2.78 \times 10^{-3} (1.33 \times 10^{-3})$
2000	$1.08 \times 10^{-3} (4.74 \times 10^{-4})$	$1.04 \times 10^{-3} (4.57 \times 10^{-4})$	$9.72 \times 10^{-4} (4.31 \times 10^{-4})$
2500	$3.44 \times 10^{-4} (1.57 \times 10^{-4})$	$3.39 \times 10^{-4} (1.54 \times 10^{-4})$	$3.29 \times 10^{-4} (1.49 \times 10^{-4})$
3000	$1.33 \times 10^{-4} (7.69 \times 10^{-5})$	$1.32 \times 10^{-4} (7.66 \times 10^{-5})$	$1.30 \times 10^{-4} (7.57 \times 10^{-5})$

Table XI. The cross section for the background (σ_B) depending on the values of invariant mass interval, the values are calculated for the process $pp \rightarrow (W^+b\bar{t} + W^-b\bar{t}) X$ at the LHC with $\sqrt{s} = 13$ TeV. The results are given in the invariant mass between $M_{Z'} - 4\Gamma_{Z'} < m_{Wbt} < M_{Z'} + 4\Gamma_{Z'}$ for different Z' decay widths.

	σ_B (pb)			
m_{Wbt} (GeV)	(for $\Gamma_{Z'_\eta}$ width)	(for $\Gamma_{Z'_\chi}$ width)	(for $\Gamma_{Z'_\psi}$ width)	(for $\Gamma_{Z'_{LP}}$ width)
$1500 \pm 4\Gamma_{Z'}$	6.60×10^{-3}	1.34×10^{-2}	5.63×10^{-3}	2.33×10^{-2}
$2000 \pm 4\Gamma_{Z'}$	1.87×10^{-3}	3.54×10^{-3}	1.50×10^{-3}	6.72×10^{-3}
$2500 \pm 4\Gamma_{Z'}$	5.26×10^{-4}	1.02×10^{-3}	4.34×10^{-4}	1.97×10^{-3}
$3000 \pm 4\Gamma_{Z'}$	1.67×10^{-4}	3.09×10^{-4}	1.33×10^{-4}	6.23×10^{-4}

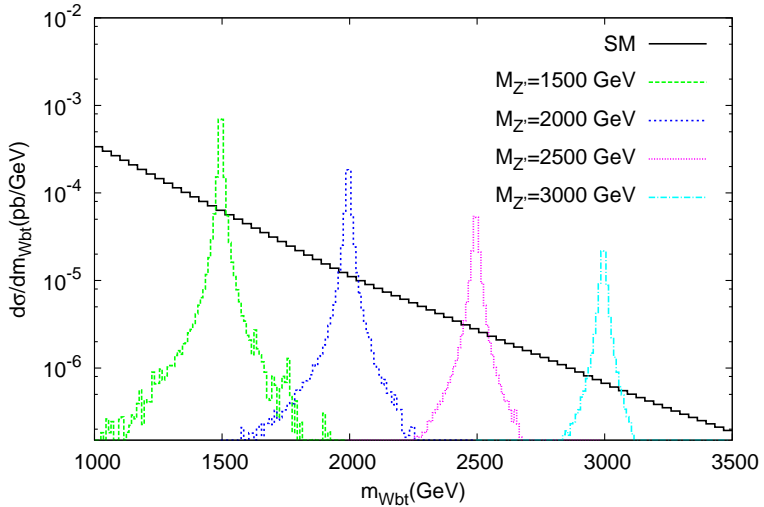


Figure 14. The invariant mass distribution of the $(W^+b\bar{t} + W^-b\bar{t})$ system for the SM and Z'_η model with different mass values of Z' boson at the LHC with $\sqrt{s} = 13$ TeV. The results are obtained for $x = 0.1$ and $m_{t'} = 700$ GeV.

cuts $|\eta| < 2$ for the central detector coverage, the results are given in Table XII, Table XIII, Table XIV and Table XV, we give the number of signal (S) and background (B) events by assuming integrated luminosity of $L_{int} = 10^5$ pb $^{-1}$ per year. For the FCNC coupling parameter $x = 0.1$, the LHC is able to measure the Z' mass up to about 3000 GeV with the associated productions of the new heavy quark t' and top quark. The statistical significance (SS) values for the final state are given in Table XII - Table XV for different Z' boson

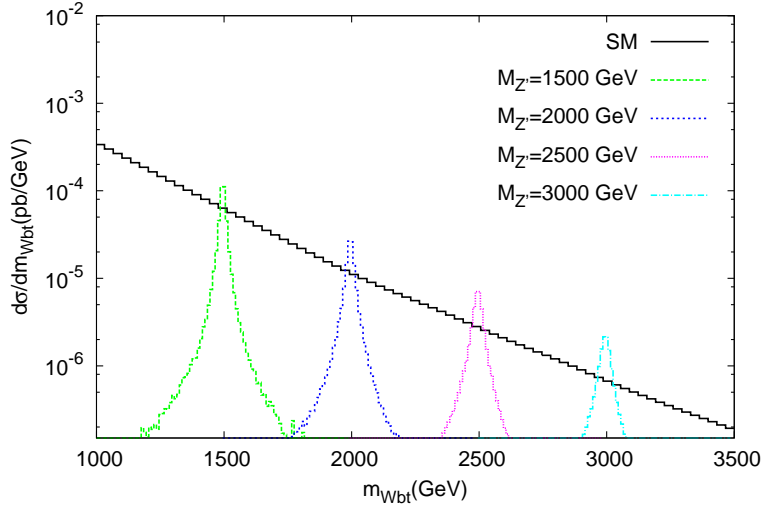


Figure 15. The same as Figure 13, but for Z'_χ model.

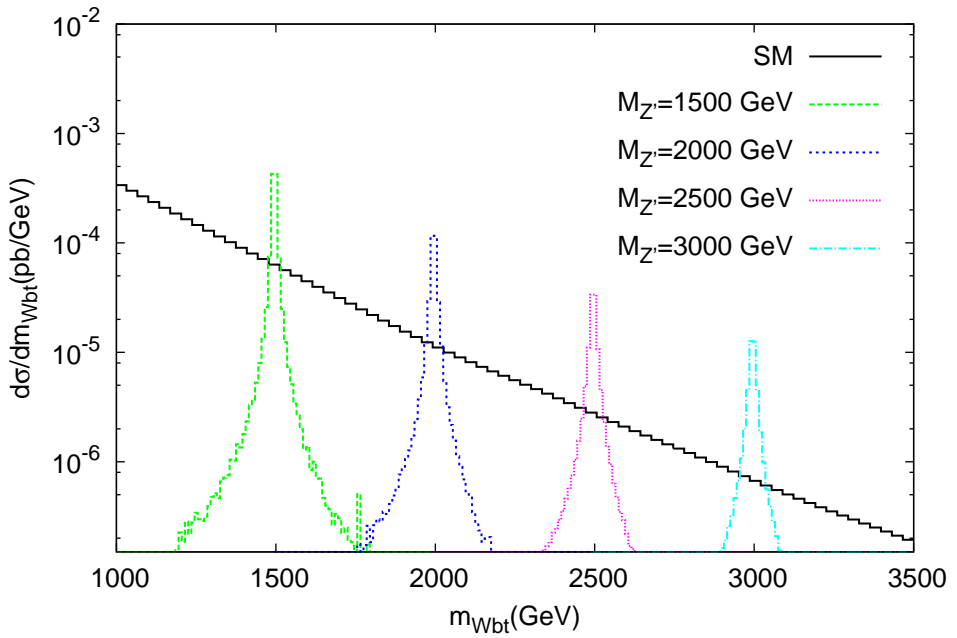


Figure 16. The same as Figure 13, but for Z'_ψ model.

masses.

In the analysis, we reconstruct the invariant mass of Wbt system around the Z' boson mass which are shown in Fig. 14, Fig. 15, Fig. 16, Fig. 17. We assume top quark decay $t(\bar{t}) \rightarrow W^+b(W^-\bar{b})$, where the W boson decays leptonically. In the final state $W^+W^-b\bar{b}$, we assume the b -tagging efficiency as 50% for each of the b -quarks. We calculate the cross section

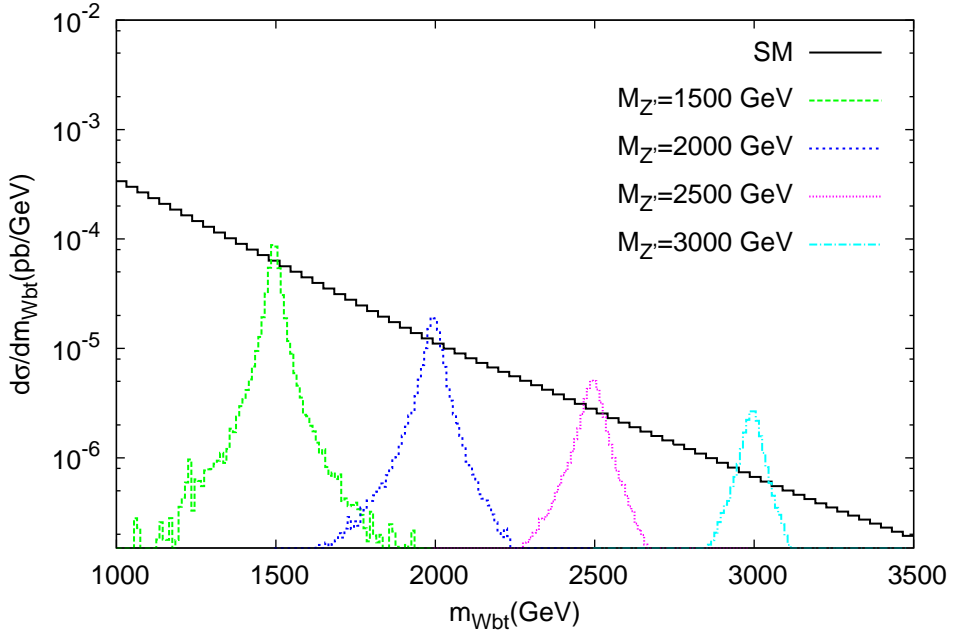


Figure 17. The same as Figure 13, but for Z'_{LP} model.

Table XII. The number of signal and background events for the final state $l^\pm + 2b_{jet} + 2jet + MET$ at the center of mass energy $\sqrt{s} = 13$ TeV and integrated luminosity $L_{int} = 10^5$ pb $^{-1}$. The numbers in the parentheses denote the signal significances (SS). These results are achieved for the Z'_η model and parameter $x = 0.1$.

	Signal - $(t'\bar{t} + \bar{t}'t) \rightarrow 2 \times (l^\pm + 2b_{jet} + 2jet + MET)$			Background - $(W^+b\bar{t} + W^-b\bar{t})$
$M_{Z'_\eta}$ (GeV)	$m_{t'} = 600$ GeV	$m_{t'} = 700$ GeV	$m_{t'} = 800$ GeV	$2 \times (l^\pm + 2b_{jet} + 2jet + MET)$
1500	305.0 (30.7)	277.8 (28.0)	245.6 (24.7)	98.6
2000	91.2 (17.3)	68.8 (16.4)	81.0 (15.3)	28.0
2500	30.0 (10.6)	29.2 (10.3)	28.0 (9.9)	7.8
3000	12.4 (7.9)	12.4 (7.8)	12.0 (7.6)	2.6

of the background in the mass bin widths for each $M_{Z'}$ value; as an example of the Z'_η model, for the $M_{Z'} = 1500$ GeV we take the invariant mass interval $\Delta m_{Wbt} \simeq 40$ GeV, and we find the background cross section $\sigma_B = 6.60 \times 10^{-3}$ pb for process $pp \rightarrow (W^-b\bar{t} + W^+b\bar{t}) + X$.

We plot the observability contours in the plane of model parameters $(x - M_{Z'})$, for different Z' models as shown in Fig. 18 at the LHC with $\sqrt{s} = 13$ TeV and $L_{int} = 100$ fb $^{-1}$. The curves with labels Z'_{LP} , Z'_χ , Z'_ψ and Z'_η show the accessible regions (below the curves)

Table XIII. The same as Table XII, but for Z'_χ .

	Signal - $(t'\bar{t} + \bar{t}'t) \rightarrow 2 \times (l^\pm + 2b_{jet} + 2jet + MET)$			Background - $(W^+b\bar{t} + W^-b\bar{t})$
$M_{Z'_\chi}$ (GeV)	$m_{t'} = 600$ GeV	$m_{t'} = 700$ GeV	$m_{t'} = 800$ GeV	$2 \times (l^\pm + 2b_{jet} + 2jet + MET)$
1500	68.0 (4.8)	61.6 (4.4)	54.8 (4.0)	200.4
2000	19.8 (2.7)	18.8 (2.5)	17.4 (2.4)	53.0
2500	6.2 (1.6)	6.0 (1.6)	5.8 (1.6)	15.2
3000	2.2 (1.4)	2.2 (1.4)	2.0 (1.4)	4.6

 Table XIV. The same as Table XII, but for Z'_ψ .

	Signal - $(t'\bar{t} + \bar{t}'t) \rightarrow 2 \times (l^\pm + 2b_{jet} + 2jet + MET)$			Background - $(W^+b\bar{t} + W^-b\bar{t})$
$m_{Z'_\psi}$ (GeV)	$m_{t'} = 600$ GeV	$m_{t'} = 700$ GeV	$m_{t'} = 800$ GeV	$2 \times (l^\pm + 2b_{jet} + 2jet + MET)$
1500	176.5 (19.2)	158.6 (17.3)	133.6 (14.6)	84.2
2000	51.3 (10.8)	49.4 (10.4)	46.4 (9.8)	22.4
2500	16.6 (6.5)	16.3 (6.4)	15.7 (6.2)	6.5
3000	6.5 (4.6)	6.4 (4.5)	6.3 (4.6)	2.0

of the model parameters at the LHC. For the Z'_η model, the FCNC parameter bounds from $x = 0.6 - 0.4$ can be searched for the mass range of $M_{Z'} = 1500 - 3000$ GeV.

V. CONCLUSION

We consider the associated productions of new heavy quark t' and top quark (with the subsequent decay channel $t' \rightarrow W^+b$) through the Z' exchange diagrams at the LHC. We

 Table XV. The same as Table XII, but for Z'_{LP} .

	Signal - $(t'\bar{t} + \bar{t}'t) \rightarrow 2 \times (l^\pm + 2b_{jet} + 2jet + MET)$			Background - $(W^+b\bar{t} + W^-b\bar{t})$
$M_{Z'_{LP}}$ (GeV)	$m_{t'} = 600$ GeV	$m_{t'} = 700$ GeV	$m_{t'} = 800$ GeV	$2 \times (l^\pm + 2b_{jet} + 2jet + MET)$
1500	77.3 (4.1)	71.5 (3.8)	64.3 (3.4)	348.5
2000	22.9 (2.3)	22.0 (2.2)	20.8 (2.1)	100.5
2500	7.6 (1.4)	7.4 (1.4)	7.2 (1.3)	29.5
3000	3.7 (1.2)	3.7 (1.2)	3.7 (1.2)	9.3

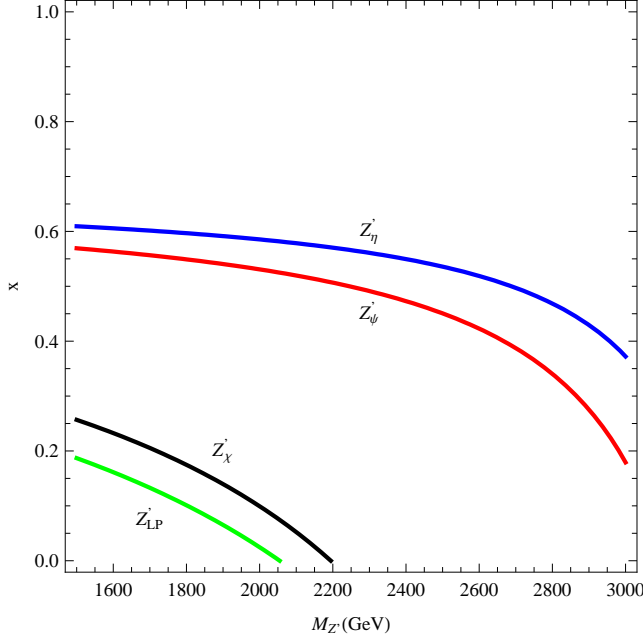


Figure 18. The contour plot for the evidence of Z' boson at the LHC ($\sqrt{s} = 13$ TeV) with $L_{int} = 100$ fb^{-1} .

find the discovery regions of the parameter space for the single productions of new heavy quarks through FCNC interactions with the new Z' boson. In the models considered in this paper, the single production of new heavy quarks at the LHC can have the contributions from the couplings of $Z'q\bar{q}$ and the FCNC couplings of $Z'q\bar{q}'$ (where $q, q' = u, c, t, t'$). For the FCNC parameter range ($0 < x < 1$ means maximal to minimal FCNC) the LHC can have the potential to produce new heavy quarks which couple to the Z' boson predicted by specific Z' models.

ACKNOWLEDGMENTS

O.C's work is supported in part by the Turkish Atomic Energy Authority (TAEK) under the project Grant No. 2011TAEKCERN-A5.H2.P1.01-19.

REFERENCES

- [1] P. Langacker, Rev. Mod. Phys. **81**, 1199 (2009).
- [2] K.A. Olive *et al.*, Particle Data Group, Chin. Phys. C 38, 090001 (2014).
- [3] A. Aad *et al.*, ATLAS collaboration, Phys. Rev. D **90**, 052005 (2014).
- [4] A. Aad *et al.*, ATLAS collaboration, JHEP **11**, 138 (2012).
- [5] S. Chatrchyan *et al.*, CMS collaboration, Phys. Lett. B **720**, 63 (2013).
- [6] S. Chatrchyan *et al.*, CMS collaboration, JHEP **04**, 025 (2015).
- [7] A. Aad et al., ATLAS Collaboration, Phys. Rev. D **88**, 012004 (2013).
- [8] S. Chatrchyan *et al.*, CMS collaboration, Phys. Rev. Lett. **111**, 211804 (2013).
- [9] A. Alves, S. Profumo and F. S. Queiroz, JHEP **1404**, 063 (2014).
- [10] A. Alves, A. Berlin, S. Profumod, F.S. Queiroz, JHEP **10**, 076 (2015).
- [11] A. Arhrib *et al.*, Phys. Rev. D **73**, 075015 (2006).
- [12] O. Cakir, I.T. Cakir, A. Senol, A.T. Tasci, Eur. Phys. J. C **70**, 295 (2010).
- [13] O. Cakir, I.T. Cakir, H.Duran Yildiz, R. Mehdiyev, Eur. Phys. J. C **56**, 537 (2008).
- [14] S. Chatrchyan *et al.*, CMS Collaboration, Phys. Lett. B **729**, 149 (2014).
- [15] A. Aad *et al.*, ATLAS Collaboration, JHEP **1411**, 104 (2014).
- [16] P. Langacker, M. Plumacher, Phys. Rev. D **62**, 013006 (2000).
- [17] K. Cheung *et al.*, Phys. Lett. B **652**, 285 (2007).
- [18] V. Barger *et al.*, Phys. Lett. B **580**, 186 (2004).
- [19] V. Barger, C. W. Chiang, P. Langacker and H. S. Lee, Phys. Lett. B **598**, 218 (2004).
- [20] C. H. Chen and H. Hatanaka, Phys. Rev. D **73**, 075003 (2006).
- [21] V. Barger *et al.*, JHEP **0912**, 048 (2009).
- [22] V. Barger *et al.*, Phys. Rev. D **80**, 055008 (2009).
- [23] A.K. Alok, S. Baek and D. London, JHEP **1107**, 111 (2011).
- [24] K. Leroux and D. London, Phys. Lett. B **526**, 97 (2002).
- [25] V. Barger, C. W. Chiang, J. Jiang and P. Langacker, Phys. Lett. B **596**, 229 (2004).
- [26] X. G. He and G. Valencia, Phys. Rev. D **74**, 013011 (2006).
- [27] C. W. Chiang, N. G. Deshpande and J. Jiang, JHEP **0608**, 075 (2006).

- [28] S. Baek, J. H. Jeon and C. S. Kim, Phys. Lett. B **641** (2006) 183.
- [29] A. Cordero-Cid, G. Tavares-Velasco and J. J. Toscano, Phys. Rev. D **72**, 057701 (2005).
- [30] C.X. Yue, H.J. Zong and L.J. Liu, Mod. Phys. Lett. A **18**, 2187 (2003).
- [31] K. Y. Lee, S. C. Park, H. S. Song and C. Yu, Phys. Rev. D **63**, 094010 (2001).
- [32] C. X. Yue and L. N. Wang, J. Phys. G **34**, 139 (2007).
- [33] F. del Aguila *et al.*, Phys. Lett. B **685**, 302 (2010).
- [34] M. Bobrowski, A. Lenz, J. Riedl and J. Rohrwild, Phys. Rev. D **79**, 113006 (2009).
- [35] A. Belyaev, N. Christensen, A. Pukhov, Computer Physics Communications **184**, 1729-1769 (2013).
- [36] J. Pumplin *et al.*, JHEP **0207**, 012 (2002).